



Imaging of shoulder instability

Massimo De Filippo¹ · Silvia Schirò² · Dani Sarohia³ · Antonio Barile⁴ · Luca Saba⁵ · Simone Cella⁶ · Alessandro Castagna⁷

Received: 28 November 2019 / Revised: 28 April 2020 / Accepted: 4 May 2020 / Published online: 23 May 2020
© ISS 2020

Abstract

The shoulder enjoys the widest range of motion of all the joints in the human body, therefore requires a delicate balance between stability and motility. The glenohumeral joint is inclined to fall into two main instability categories: macro and micro. Macroinstability can be traumatic or atraumatic, with anterior or posterior dislocation of the humeral head. Microinstability falls within the broader section of acquired instability in overstressed shoulder caused by repeated joint stress. Anterior traumatic instability is the most frequent entity and a relatively common injury in young and athletic population. While shoulder instability is a clinical diagnosis, imaging impacts the patient management by detailing the extent of injury, such as capsulo-labral-ligamentous tears, fracture, and/or dislocation, describing the predisposing anatomic conditions and guide the therapeutic choice. The aim of this comprehensive review is to cover the imaging findings of shoulder instability by different imaging techniques.

Keywords Shoulder instability · Magnetic resonance arthrography · Computed tomography arthrography · Shoulder anatomic variant

Introduction

The shoulder is the most mobile joint in the human body [1, 2]. The anatomy of the glenohumeral joint is complex, relying on both static and dynamic stabilizers to maintain a delicate balance between free range of motion and joint stability [3, 4].

The shoulder is an imperfect ball-and-socket joint: the socket (glenoid) is smaller in size than the ball (humeral head)

but has a larger radius of curvature. This anatomy lends itself to extraordinary mobility, yet increases the risk of dislocation [2].

Glenohumeral instability is divided in two main categories: shoulder macroinstability and microinstability. The former includes several clinical entities, which can be classified in two groups based on biomechanical and clinical criteria [5]: (i) traumatic etiology, *unidirectional instability*, *bankart lesion*,

Electronic supplementary material The online version of this article (<https://doi.org/10.1007/s00256-020-03459-z>) contains supplementary material, which is available to authorized users.

✉ Massimo De Filippo
massimo.defilippo@unipr.it

Dani Sarohia
dasahoria@ucdavis.edu

Luca Saba
lukas_red@hotmail.it

Simone Cella
scella@ao.pr.it

¹ Department of Medicine and Surgery (DiMec), Section of Radiology, University of Parma, Maggiore Hospital, Via Gramsci 14, 43126, Parma, Italy

² Department of Medicine and Surgery (DiMeC), Section of Radiology, University of Parma, Via Gramsci 14, 43126 Parma, Italy

³ Department of Radiology, University of California Davis, 4860 Y Street, Sacramento, CA 95817, USA

⁴ Department of Biotechnological and Applied Clinical Sciences, University of L'Aquila, Ospedale San Salvatore, L'Aquila, Italy

⁵ Department of Radiology and Nuclear Medicine, Centre Henri Becquerel, Rue D'Amiens, 76000 Rouen, France

⁶ Department of Medicine and Surgery, Unit of Radiologic Science, University of Parma, Maggiore Hospital, Via Gramsci 14, Parma, Italy

⁷ Shoulder Unit, Humanitas Research Hospital, Via Manzoni 56 Rozzano, Milan, Italy

surgery (TUBS) and (ii) atraumatic or minor trauma, multidirectional instability, bilateral, rehabilitation, inferior capsular shift (AMBRI); the latter falls within the broader section of acquired instability in overstressed shoulder (AIOS), or acquired instability caused by repeated joint stress in forced abduction-external rotation of the arm.

Instability of the shoulder may cause dysfunction and pain, especially in dynamic activities affecting the quality of life: initially, the structural damage is reversible and characterized by contusion and strain of the ligaments. Later it may lead to severe anatomic damage including rotator cuff tear and arthritis.

Joint instability is often confused with laxity; however, they are two different conditions. The latter is characterized by a physiological looseness of the capsuloligamentous structures and generally does not result in pain [2, 6–8]. It does however increase the risk of instability.

Shoulder instability is a clinical diagnosis; however, radiologic imaging significantly enhances the clinical management by depicting the injury's extent, including fracture and/or dislocation, and may detect the predisposing anatomical conditions [6–8]. The purpose of this review article is to describe the role of different imaging modalities in the diagnosis of shoulder instability.

Background

Static stabilizers

Morphology of the articular bone interface The extent of the contact area and the angle degree between the humeral and glenoid surfaces significantly affects joint congruity. The glenoid is pear-shaped or oval-shaped on sagittal sections. Three main shapes of the glenoid surface are described in literature: concave, flat, or convex. Moreover, acquired factors leading to the reduction of the glenoid (i.e., bony Bankart) or humeral bone surfaces (i.e., Hill-Sachs lesion) are an important cause of stability loss.

Glenoid labrum It is a fibrocartilaginous structure that fits along the edge of the glenoid cavity extending the size, the depth, and the area of contact with the humeral head creating a “vacuum effect.” The glenoid labrum also constitutes a valuable anchor for the joint capsule, the glenohumeral ligaments, and the tendon of the long head of the biceps muscle [4, 9].

The labrum adheres firmly to the edge of the glenoid surface under the equatorial plane where it appears rounded, and less firmly to the upper portion of the glenoid surface where it has a typical triangular shape. Lesions of the glenoid labrum reduce the depth of the glenoid and compromise the anchorage of capsule and glenohumeral ligaments, resulting in a reduction of joint stability [4, 9].

Capsuloligamentous structure It is made of a thin fibrous tissue from the periphery of the glenoid labrum, surrounding the glenohumeral joint to the anatomical neck of the humerus. This structure is reinforced anteriorly by three glenohumeral ligaments, divided into superior, middle, and inferior ligaments. The latter is actually defined as an inferior ligamentous complex including anterior and posterior bands.

Intra-articular negative pressure and cohesive forces of the synovial fluid The glenohumeral joint can be assimilated to a closed compartment in which the negative pressure along with the cohesive forces of the synovial fluid creates a “vacuum effect.” This enhances the adhesion of the joint.

Dynamic stabilizers

Muscular structures located in the shoulder girdle (n26) The most relevant are subscapularis, supraspinatus, infraspinatus, and teres minor (which constitutes the “rotator cuff”), and the long head of the biceps muscle [4, 6, 9].

Anatomic variants

Many anatomical variants of glenoid and of the capsular-labral complex are found. The misinterpretation of these variants may potentially lead to diagnostic errors [10].

Glenoid

The posteroinferior edge of the glenoid can present several normal shapes such as triangular, rounded, and j or delta-shaped. The j or delta-shaped rim variants can be associated with varying degree of posterior shoulder instability due to loss of concavity. The tubercle of Assaki is a plica of the subchondral bone, situated in the center of the glenoid cavity. It is associated with a focal thinning of the overlying cartilage. This should not be mistaken for a cartilage defect. A bare area has also been described in the mid third of the glenoid cavity; this is an oval area denuded of cartilage, probably a developmental error and should be differentiated from true cartilage injury.

Glenoid dysplasia embraces an osseous hypoplasia of the posteroinferior glenoid edge that presents a slopped and flattered shape. Commonly, it is associated with hypertrophy of contiguous cartilage, labrum, and glenoid irregularity. This variant may lead to shoulder instability [11].

Capsular-labral complex

To ease with the localization of both labral lesions and anatomical variants, Resnick D. adapted the glenoid surface to a clock face; conventionally, it's divided into four or six parts. According to this subdivision, the upper portion corresponds

to 12 o'clock, the lower portion to 6 o'clock, and the anterior and posterior portions respectively to 3 and 9 o'clock and to 9 and 3 o'clock for right and the left shoulder, respectively. According to the described scheme, the most frequent anatomical variants fall between 11 and 3, and include the sublabral recess, the sublabral foramen, and the "Buford complex" (supplemental Fig. 1) [12, 13].

The sublabral recess is a groove located between the labral-bicipital complex and the upper portion of the glenoid cartilage between 11 and 1 (Fig. 1b). It usually measures 2 mm in width. The sublabral recess is best seen on MR arthrography using fat-saturated T1-weighted oblique coronal images and it extends medially towards the glenoid. This anatomical variant should not be mistaken for a SLAP tear (see "Shoulder microinstability"), i.e., type II.

The sublabral foramen is a gap between the anterosuperior portion of the glenoid labrum and the adjacent glenoid cartilage. It is generally between 1 and 3, anterior to the labral-biceps complex (Fig. 1c) [10]. The sublabral foramen provides a communication between the glenohumeral joint and the subscapularis recess. It is best seen fat-saturated T1-weighted oblique coronal images obtained with MR arthrography. The sublabral foramen should not be mistaken for anterosuperior labral tear especially in symptomatic patients.

The "Buford complex" is the absence of the superior anterior glenoid labrum (between 1 and 3) associated with a cord-like middle glenohumeral ligament as can be observed in MR arthrography (Fig. 2) [12, 13]. The thickened middle glenohumeral ligament attaches directly on the anterosuperior glenoid and may be mistaken for a displaced labral foramen. These anatomical variants involve primarily the anterior capsular insertions. Three types of capsular insertion have been described depending on the distance of capsular insertion from the glenoid margin (Fig. 3). In *type I*, the capsule appears to attach to the glenoid margin and labrum. In *type II*, the capsule attaches to the glenoid neck ≤ 1 cm of the labrum. In *type III*, the attachment is ≥ 1 cm medial to the labrum. Only type III (supplemental Fig. 3c) with medial anterior capsular insertion can lead to instability.

Shoulder instabilities are typically divided into macro- and microinstabilities, based on their anatomical and clinical

features [2, 14, 15]. However, the spectrum of shoulder instability is very wide, and many classifications have been proposed. The most complete classifications are Matsen [5, 16], Gerber [17] and Stanmore [18]. For simplicity, we will follow the Matsen classification because it includes most of the pathological findings related to glenohumeral instability.

Shoulder macroinstability

Shoulder macroinstability includes different clinical entities. These are classified into two groups following the etiopathogenetic features and possible therapeutic options [19].

Traumatic instability/traumatic etiology, unidirectional instability, Bankart lesion, surgery required [19, 20] The glenohumeral dislocation is frequently anterior-inferior-medial (95% of cases) and less frequently in other directions (3% posterior, 1% multidirectional) [5].

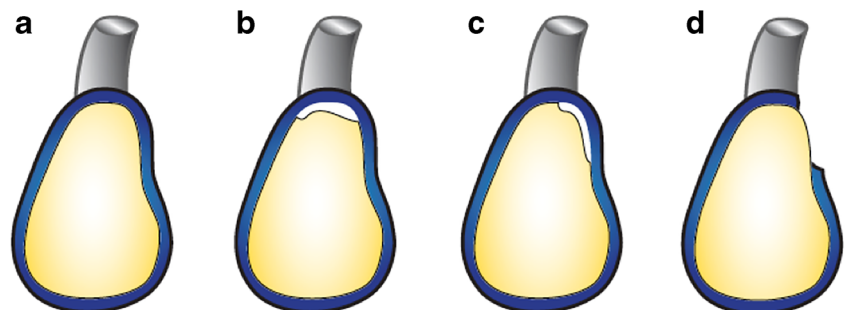
The likelihood of a recurrent dislocation episode following traumatic lesions of the shoulder is inversely proportional to the age of the patient. Thus, young patients have a greater probability of shoulder re-dislocation after traumatic lesions [20].

Traumatic shoulder dislocations are often associated with lesions of the fibrocartilaginous labrum specifically involving the anterior and inferior portions (between 3 and 6 in the right shoulder and between 6 and 9 in the left shoulder).

The following types of labral-ligamentous complex lesions are associated with traumatic instability (Fig. 4):

- Bankart lesion (supplemental Fig. 4a) is the most typical and frequent lesion. It consists of the complete avulsion of the labrum from the glenoid in the subequatorial region with rupture of the periosteum. This detachment reduces the strain of the middle and inferior glenohumeral ligaments, which lose their effect [21].
- Perthes lesion (supplemental Fig. 4b) is characterized by the complete avulsion of the labrum with stripped but intact periosteum (periosteal sleeve).

Fig. 1 a–d Schematic view of glenoid fibrocartilage. **a** Normal glenoid fibrocartilage; **b** at 11–1 sublabral recess; **c** at 1–3 sublabral foramen; **d** at 1–3 Buford complex



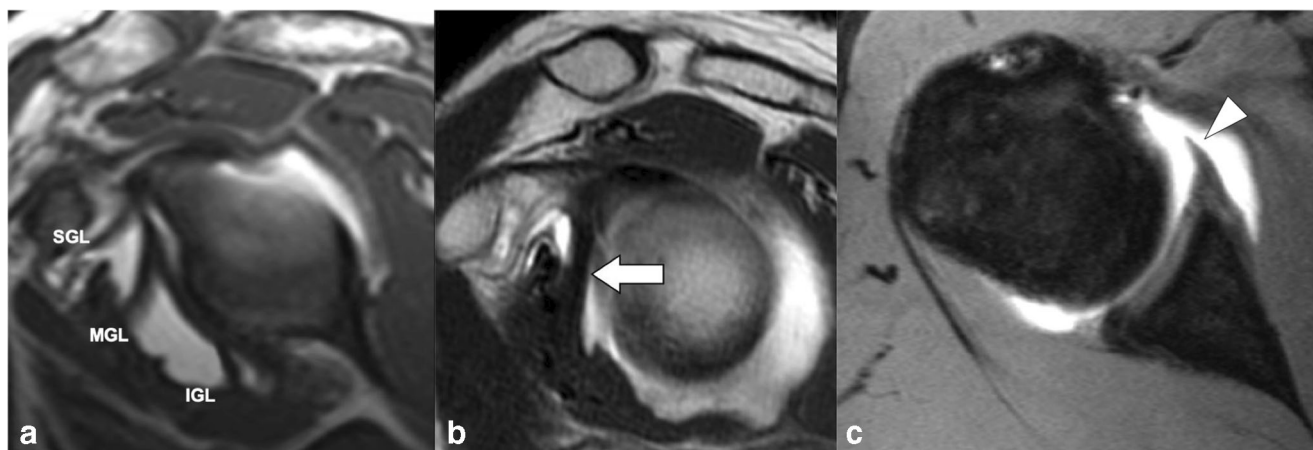


Fig. 2 a–c MR arthrography. **a** Sagittal T1w image shows an overall view of glenohumeral ligaments (superior: SGL, middle: MGL, inferior: IGL); **b** Buford complex; note the “cord-like” middle

glenohumeral ligament (arrow) and absence of the anterosuperior labrum; **c** axial T1w fat-suppressed image showing the anterior band of the IGL insertion at the anterior labrum (arrowhead)

- ALPSA lesion (anterior labroligamentous periosteal sleeve avulsion) (supplemental Fig. 4c) is the outcome

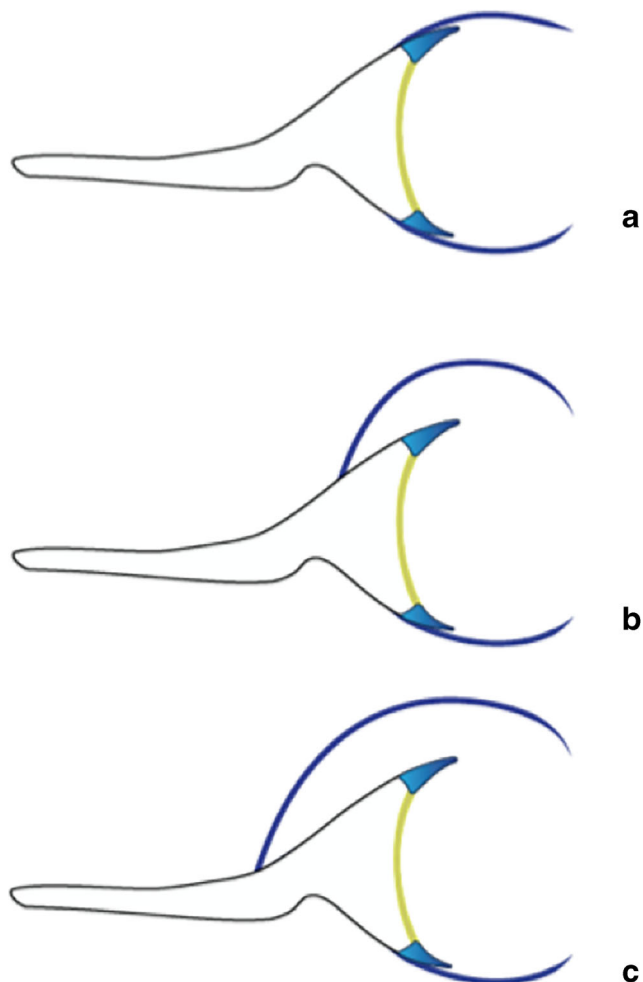


Fig. 3 a–c Schematic view showing variants of anterior capsular insertion: **a** type I; **b** type II; **c** type III. Type III is a predisposing condition to anterior shoulder dislocation

of a Perthes lesion with retraction of the periosteum. The periosteum remains intact but detaches from glenoid, allowing the anterior labroligamentous complex to displace medially and to rotate inferiorly to the scapular neck. If untreated, this injury can result in a scarred deformed labrum which results in joint instability [22].

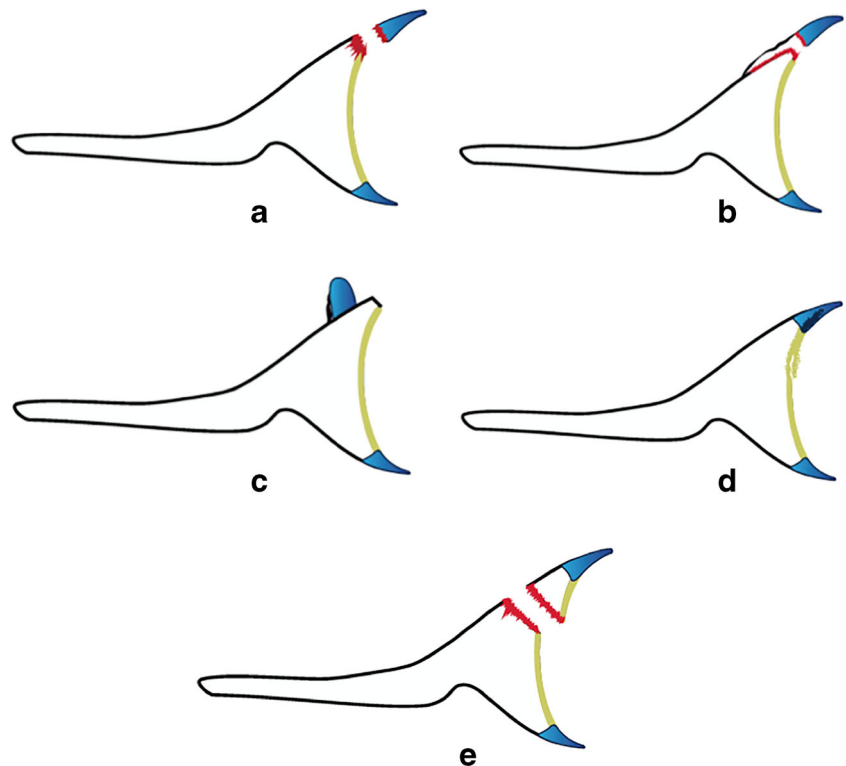
- GLAD lesions (glenolabral articular disruption) (supplemental Fig. 4d) consist of a superficial anteroinferior glenoid labrum lesion with intact periosteum associated with cartilage erosion of the corresponding region of the glenoid cavity [23, 24]. Unlike the Bankart lesions, the GLAD lesions are generally the result of compression rather than shearing. Occasionally, it is associated with anterior instability [23, 24].
- Humeral avulsion of the glenohumeral ligament (HAGL) and reverse-HAGL both involve the avulsion of the inferior glenohumeral ligament, the most important anterior stabilizer of the shoulder [25]. These conditions are very difficult to recognize and are commonly missed on magnetic resonance imaging (MRI).

A scar-fibrotic retraction of the anteroinferior glenoid labrum due to several dislocations can cause the “Glom Sign” (glenoid ovoid mass), a fibrotic small mass anteromedial to the glenoid. Labrum lesions may be associated with osseous findings, especially in major trauma [26].

In anterior shoulder dislocation, the posterolateral superior region of the humeral head commonly collides with the antero-inferior glenoid. This is the leading mechanism of Hill-Sachs impaction fracture of the humeral head.

The Hill-Sachs lesion is seen as a focal concavity or defect with subjacent bone edema along the posterolateral superior humeral head, best demonstrated on axial images [26, 27]. This type of lesion not only indicates antero-inferior dislocation but also provides useful insights into shoulder stability

Fig. 4 a–e Schematic view of labral lesions: **a** Bankart lesion complete avulsion of the labrum from the glenoid in the subequatorial region with rupture of the periosteum; **b** Perthes lesion complete avulsion of the labrum with stripped but intact periosteum; **c** ALPSA lesion outcome of Perthes lesion with retraction of the periosteum.; **d** GLAD superficial anteroinferior glenoid labrum lesion with intact periosteum; **e** Bony Bankart lesion fracture of the anteroinferior glenoid rim along with the labral avulsion



before the dislocation [3, 26]. Especially, the depth of Hill-Sachs fracture can help distinguish stable joints from unstable joints [27–29]. Hill-Sachs lesions usually have a vertical orientation and do not affect the recovery of stability. However, when Hill-Sachs lesions are horizontally oriented, in particular when the superior humeral head is involved, they may be associated with high rate of recurrent dislocation after arthroscopic treatment.

Several methods are currently available in order to assess the depth of Hill-Sachs lesion. A quantitative measurement can be made using anteroposterior (AP) plain radiographs calculating the P/R ratio (normal value $r = 0.27$) between the maximum depth of the notch defect (P) in internal rotation and the radius (R) of the humeral head. Another method is based on 3D computed tomography (CT) reconstructions. Using this method, an accurate evaluation of the size (width and depth measured on axial and coronal images), orientation (Hill-Sachs angle), and location (bicipital and vertical angles) of the Hill-Sachs lesion can be made [30]. The Hill-Sachs angle has been defined by Cho et al. as the angle between the line passing through the deepest groove of the Hill-Sachs lesion and the longitudinal axis of the humeral shaft on the true posteroanterior on 3D CT [30].

The bicipital angle has been defined as the angle between the line connecting the center of the humeral head to the center of the bicipital groove and the line connecting the center of the humeral head to the center of the Hill-Sachs lesion on axial CT image [30].

Violent traumas can be linked to another type of bone lesion, the “bony Bankart,” or fracture of the anteroinferior glenoid rim along with the labral avulsion (supplemental Fig. 4e). To evaluate the shoulder stability in the presence of bipolar bone loss that involves both the glenoid and the humeral head, Yamamoto et al. proposed the “glenoid track” concept [31].

The glenoid track is defined as the contact surface of the humeral head with the glenoid when the shoulder is in abduction and external rotation. Di Giacomo et al. extended this concept to evaluate the engagement of Hill-Sachs lesions on the glenoid rim with or without the presence of anterior glenoid bone loss. Therefore, if the Hill-Sachs lies within the glenoid track (on-track), no engagement/dislocation occurs. On the other hand, if the Hill-Sachs lesion lies beyond the glenoid track (off-track), the engaged anterior rim of the glenoid may fall into the Hill-Sachs causing new dislocation [32, 33]. The method proposed by Di Giacomo et al. in order to assess an on-track/off-track Hill-Sachs lesion on CT Volume Rendering (VR) is showed in Fig. 5.

The most common and effective procedure performed in patients with engaging Hill-Sachs lesions (off-track) is the arthroscopic “remplissage.” The procedure consists of posterior capsule/infraspinatus tenodesis fixed into the Hill-Sachs defect, in order to fill in the gap of depressed bone [34].

Posterior traumatic instability of the shoulder is less frequent than anterior, and accounts for less than 5% of total shoulder dislocations [28]. Posterior instability can be characterized by the presence of isolated lesions of the labrum,

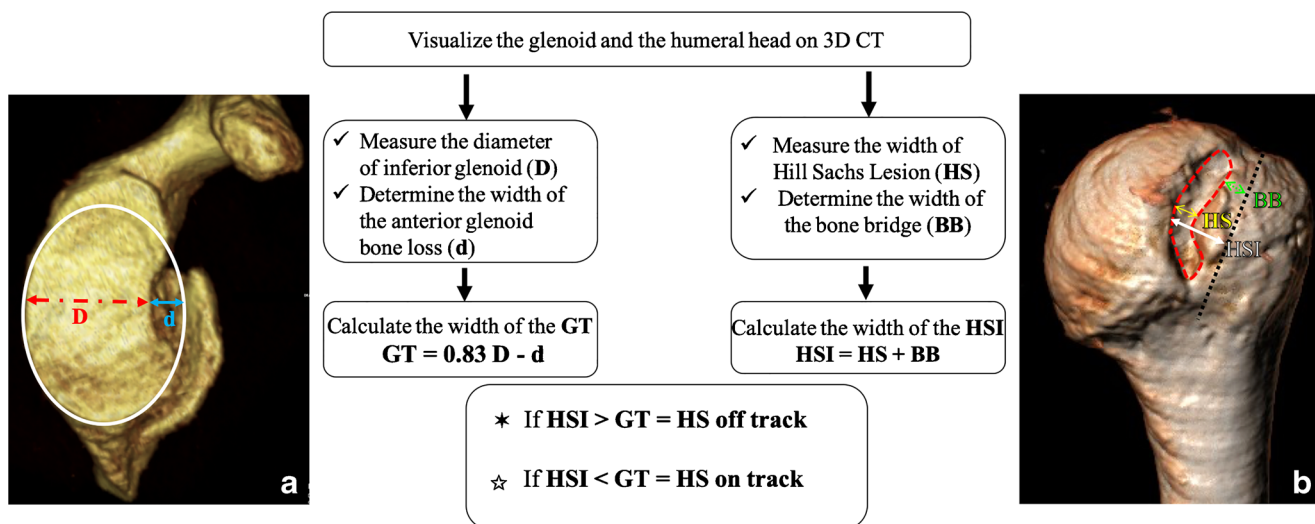


Fig. 5 Flow chart illustrating how to measure on-/off-track lesion along with **a** CT 3D VR reconstruction of the glenoid bone showing how to measure the glenoid track and **b** CT 3D VR reconstruction of the humeral head showing how to measure the Hill-Sachs Interval (HSI). In **a**, red dotted arrow represents the diameter of the inferior glenoid (**D**); light blue arrow corresponds to the width of the anterior glenoid bone loss (**d**). In **b**,

black dotted line represents the medial margin of the rotator cuff attachment; yellow arrow symbolizes the width of the Hill-Sachs lesion (**HS**); green dotted arrow corresponds to the width of the bone bridge defines the intact bone that lies between the Hill-Sachs lesion and the posterior rotator attachments cuff (**BB**); white arrow represents the Hills Sachs interval (**HSI**)

capsular distension, complex lesions with detachment of capsule-periosteum or bone lesions of the posterior glenoid (erosions or fractures called “bony Bankart reverse”), and/or impact fractures of the humeral head (type MacLaughlin or reverse Hill-Sachs) [28, 35].

Atraumatic instability/atraumatic or minor trauma, multidirectional instability, bilateral, rehabilitation, inferior capsular shift (AMBRI) [4, 20] Atraumatic, multidirectional, generally bilateral, its initial treatment is rehabilitation and only secondarily, arthroscopy with capsuloplasty [4, 19, 20]. The etiopathology is due to the redundancy of the capsule-ligamentous complex, which is a primary intrinsic stabilizer of the shoulder (wide capsule or anterior capsular very medial) and affects both shoulders [19]. The concept of “multidirectional instability” is very much controversial in the orthopedic community as an entity that is not easily defined and understood. As already mentioned, this kind of instability does not show major structural lesions. Capsular redundancy and/or blunt/rounded labrum is the only findings as can be observed in MR arthrography (Fig. 6).

Capsular volume and anatomic description are relevant for the treatment planning. Commonly, subjects with AMBRI show increased joint capsular volume given by elongated inferior capsule and deficient rotator interval. Park et al. described a MR arthrography method in order to accurately evaluate the capsular volume defined by the glenocapsular (GC) ratio [36].

In order to measure the GC ratio, the oblique coronal fat-suppressed T1-weighted image containing the largest glenoid cut and the insertion of the biceps long head should

be chosen. Widths from the superior aspect of the glenoid to the most inferior aspect of the capsule (A), as well as those from the superior aspect of the glenoid to the most inferior aspect of the glenoid should be recorded (B). Therefore, the GC ratio is calculated by dividing A by B. Interestingly, the GC ratios are significantly larger in the patients with AMBRI.

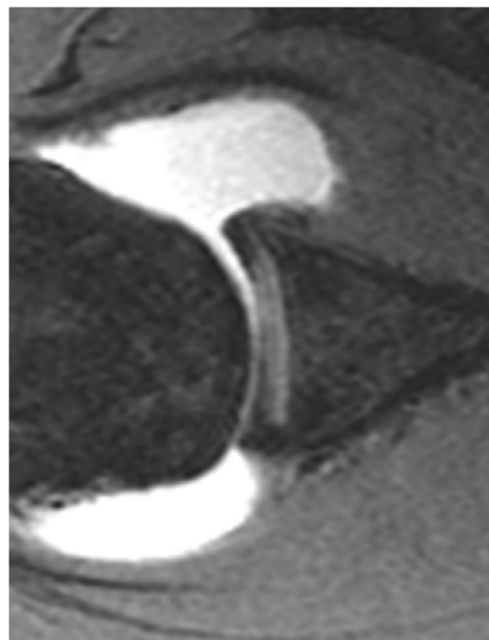


Fig. 6 AMBRI (atraumatic or minor trauma, multidirectional instability, bilateral, rehabilitation, inferior capsular shift). Axial SE T1 SPIR MR Arthrography image shows absence of the anterior and posterior labrum

Shoulder microinstability

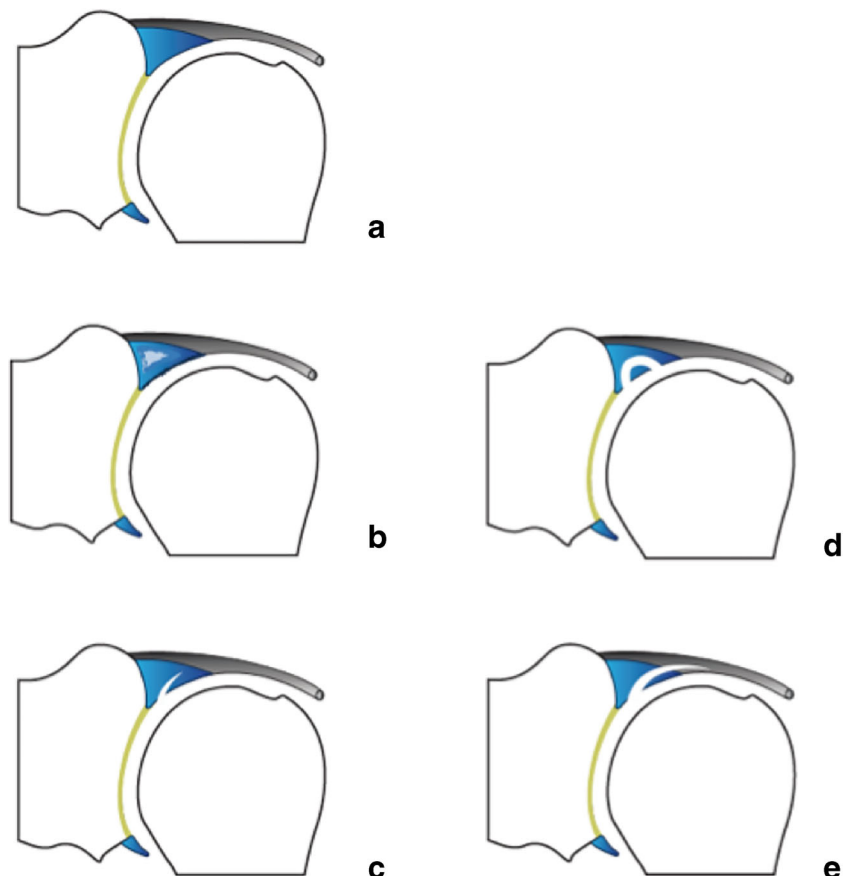
Microinstability of the shoulder falls within the broader section of AIOS (*acquired instability in overstress shoulder*), or acquired instability caused by repeated joint stress in forced abduction-external rotation of the arm [2, 14, 20, 37, 38].

Usually these instabilities affect over-head athletes (basketball, volleyball, swimming, tennis, baseball, etc.) and workers whose job requires frequent raising of the elbow above the shoulder [5, 14, 19, 20]. These patients report insidious pain that prevents abduction and external rotation of the humerus [19, 20]. In this type of instability, there is a progressive failure of anterior capsular and lower and middle glenohumeral ligaments that compromise the restraint function of the capsuloligamentous complex [5, 20]. In some cases, during the throwing motion, a slight anteroinferior translation of the humeral head with respect to the glenoid cavity causes an abnormal contact between the articular surface of the supraspinatus tendon and the posterosuperior glenoid labrum, resulting in an “internal impingement” or “posterosuperior impingement” [39].

The group of microinstability includes the SLAP lesions (*superior labrum anterior to posterior*), or lesions of the glenoid labrum above the equatorial region, where the tendon of the long head of the biceps is located (Fig. 7) [2, 40]. Great

attention has been paid over the years to this type of injury, due to its common occurrence in young athletes [41]. The first classification was proposed by Snyder et al. in 1990 [42]. This divides the SLAP lesions into four types by arthroscopic assessments; subsequently, several studies have shown a good correlation between arthroscopy and MR arthrography in the diagnosis and classification of SLAP lesions [41–44]. The type I (Fig. 7b) is characterized by friability, without real break of the articular surface of the upper portion of the glenoid labrum, with regular insertion of the long head of the biceps. The type II (Fig. 7c) consists of a detachment of the upper portion of the labrum and does not affect the insertion of the long head of the biceps. The type III (Fig. 7d) is characterized by “bucket handle” lesion of the upper portion of the labrum, with the central part displaced into the joint, and the peripheral portions welded to the glenoid margin. This type of injury does not affect the long head of the biceps. The type IV (Fig. 7e) is the type III with involvement of biceps tendons. Literature reports different level of incidence for each type of SLAP tear [45–47]. An incidence of 9.5–21% is reported for type I; 41–55% for the type II; 6–33% for the type III; and 3–15% for the type IV. Type II is the most frequent lesions identified in arthroscopy; similar prevalence is found with MR arthrography [47]. Another classification distinguishes SLAP lesions in 12 degrees; it is based on the

Fig. 7 a–e Schematic view of SLAP lesion (*superior labrum anterior to posterior*), or lesions of the glenoid labrum above the equatorial region with involvement of the biceps tendons. **a** Normal. **b** Type I, friability without a tear. **c** Type II, detached upper portion of the labrum, without affecting biceps tendon. **d** Type III, bucket handle lesion of the labrum. **e** Type IV, type III with involvement of biceps tendons



association of lesions reported in Snyder's classification with subequatorial lesions of the glenoid fibrocartilage, anterior and posterior [42].

Shoulder dislocations can be caused by instability of the extra- and intra-articular portion of the long head of the biceps, as shown in MR arthrography (Fig. 8). A consequence of the microinstability is the rotator interval cuff tear, a pre-insertional tendinosis of the long head of the biceps, characterized by thickening and hyperintense signal on MR T1 SPIR-weighted images (Fig. 9).

Radiological imaging

Conventional radiography

Conventional radiography (CR) represents the first line of investigation in shoulder instability [48]. Correct assessment of routine plain films constitutes a guide for choosing further imaging methods. A proper technical execution of radiographic examination is essential for an accurate assessment of the glenohumeral bone component [48]. Commonly, at least two perpendicular planes' projections including the affected region should be obtained in order to assess shoulder instability. Standard series of shoulder plain films in suspicion of instability should include AP and true anteroposterior view according to Grashey (posterior oblique at 40°, true being with respect to the glenohumeral joint space) projections, axillary view, and the modified scapular Y view ("outlet" view). When "outlet" radiographs are combined with true AP and lateral axillary radiographs, three different views that are perpendicular to each other are obtained, and the level of information that may be achieved with plain films reaches the maximum.

Additional views may be obtained in specific pathologic conditions of the shoulder region such as Bernageau's view and Stryker-Notch's view.

Fig. 8 a–b Axial T1 w Fat-suppressed MR images of two different patients showing dislocation of the long head of biceps tendon in the extra-articular portion (a, arrow) and the intra-articular portion (b, arrow)

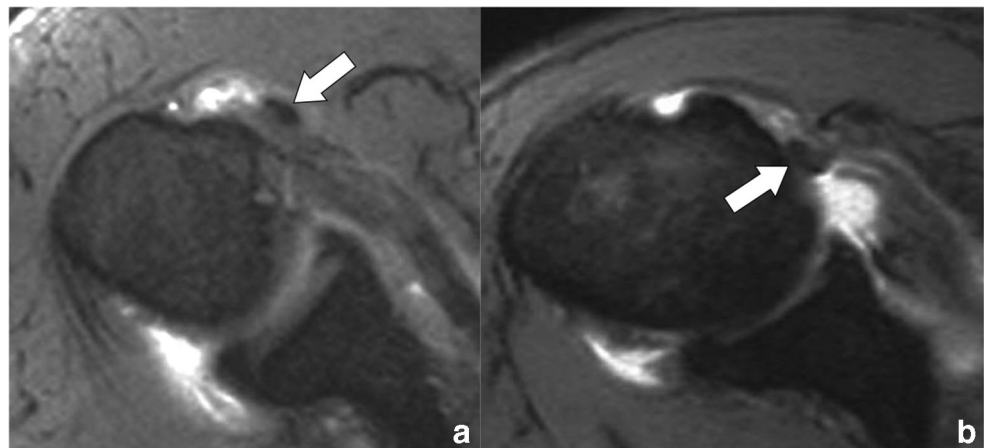


Fig. 9 Sagittal SE T1 SPIR MR arthrography image shows rotator interval cuff, in particular the coracohumeral ligament (arrowhead) and the superior glenohumeral ligament (asterisk). The pre-insertional long head of the biceps shows high signal intensity (arrow) due to tendinosis. This condition is often consequent to a microinstability of the intra-articular portion of the tendon

Anteroposterior view

Commonly, two AP plain films are obtained where the arm is either rotated internally or externally. As the glenohumeral joint is aligned anterolaterally on a 35°–40° angle, the glenoid rim and the humeral head overlap on these images (Fig. 10); therefore, only the humeral head is displayed from two different directions on these images. However, a single AP radiograph in a neutral position of the arm along with the other standards' projection is sufficient to find out anterior dislocation. In this view, if the observer will see inferior and medial dislocation of the humeral head with respect to the glenoid (or in the axillary joint recess), an anterior dislocation should be suspected. Anterior dislocation is going to be apparent in the AP view, but posterior dislocation can be missed in non-experienced radiography readers.



Fig. 10 CR, anterior shoulder dislocation. A-P view is generally sufficient for the diagnosis of anterior shoulder dislocation; it shows the inferior and medial dislocation of the humeral head with respect to the glenoid (or in the axillary joint recess)

Grashey view: the true AP radiograph of the shoulder

As the scapula is located at the superior posterolateral part of the chest, the actual AP radiograph of the glenohumeral joint is obtained by administering X-rays with an angle of 45° from the medial aspect towards the lateral direction. These plain films may be obtained in the supine or standing position. The major advantages of the actual AP- Grashey projection over conventional AP radiographs are outlining the glenohumeral joint and characterizing the glenoid clearly from the humeral head (Fig. 11). If the humeral head overlaps the

scapular glenoid on this projection, it means that the glenohumeral joint is dislocated either anteriorly or posteriorly. Grashey view is the most valuable for the diagnosis of fractures of the coracoid, glenoid, and proximal humerus but mainly for posterior glenohumeral instability.

Axillary view (west point view)

The axillary view displays the relationship between the humeral head and glenoid in detail. It is used for the diagnosis of glenohumeral joint dislocation. Abduction of the arm to a level of 70° – 90° is a must in a supine or standing patient. It improves the detection of a Bankart fracture of the anterior glenoid rim [32, 49]. It is also useful in showing dislocations, subluxations, or compression fractures (including Hill-Sachs lesions) of the humeral head and anterior or posterior glenoid rim fractures. In acute trauma, abduction of the arm may be challenging to obtain; therefore, this projection may not be possible in the ER. In these cases, modified axillary radiographs (Velpeau axillary lateral projection, Stripp axial lateral projection, trauma axillary lateral projection) or scapular Y radiographs can replace this view.

“Outlet” (modified scapular Y) view

“Outlet” radiographs reveal a cross-section of the exit (outlet) of supraspinatus towards the arm and highlight clearly the relationship between the subacromial space and the acromion by revealing the undersurface of the acromion. In the “outlet” view, there is an overlap of the coracoacromial curve, and the curve formed by the scapular body and spine. It allows profiling the undersurface of the acromion in order to provide important information



Fig. 11 a–c CR true A-P view or Grashey view images, c magnified view of b with anatomy defined. In a, the radiolucent glenohumeral space indicates the regular anatomical relationships. In b–c, the intersection of

the profiles of the scapular glenoid and humeral head is a radiographic sign of posterior dislocation of the shoulder (“crossover sign”)

for surgical intervention (acromioplasty). The outlet view is a variation of the scapular Y projection that is commonly used. In case of painful shoulder, accurate positioning is not needed. It may be obtained while the arm is in medial rotation in an arm support. Hence, acquiring this view in acute trauma is easier than a lateral axillary radiograph, a real lateral view of the scapula and the lateral aspect of the glenohumeral joint will be observed. Lateral projection of the scapula forms the letter “Y.” Upper arms of the Y are formed by the coracoid process anteriorly and the scapular spine posteriorly. The vertical arm of the letter is the body of the scapula. The glenoid fossa is located at the intersection of the three arms. The head of the humerus overlaps the glenoid fossa in a normal shoulder. Medial and lateral borders of the scapula overlap each other at a successfully positioned Y radiograph. Y radiographs particularly exhibit the relation between the humeral head and the glenoid fossa at an oblique sagittal plane. While the humeral head is displaced to the anterior (or, more precisely, commonly anteroinferior) aspect of the glenoid fossa during anterior shoulder dislocations, it is displaced posteriorly with respect to the glenoid fossa during posterior dislocations. Scapulolateral radiographs do not show the fractures of anterior or posterior glenoid rim, but determination of displaced fractures of the greater tubercle of the humerus is possible. It provides information about dislocation of the shoulder and fractures of the proximal humerus or the scapula. Hill-Sachs lesions are seen more clearly on the Y view than on lateral axillary radiographs.

Additional projections

Bernageau’s view

This view shows the glenohumeral alignment in the axial plane like a true tangential view. It is particularly useful for the diagnosis of the anterior subluxation of the shoulder (Fig. 12). Moreover, it provides an optimal visualization of the anteroinferior segment of the glenoid rim that especially in patients with anterior instability is usually damaged. (Fig. 12). [20, 49, 50].

Stryker-Notch’s view

Stryker-Notch’s view is useful for patients with recurrent shoulder dislocation (Fig. 13). This view demonstrated the posterolateral aspect of the humeral head and is excellent for depicting Hill-Sachs lesions or the flattening of the posterolateral humeral head. However, evaluation of the glenoid rim fractures or subtle glenohumeral subluxation is limited.

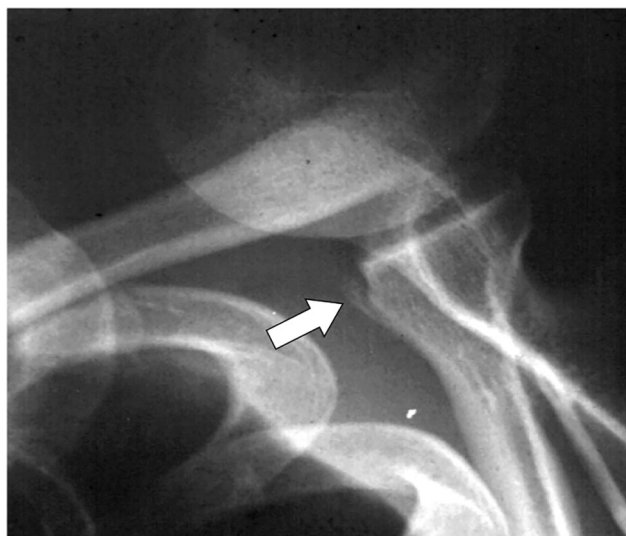


Fig. 12 CR, Bernageau’s view shows the glenohumeral joint in the axial plane and is particularly useful for the diagnosis of shoulder subluxation and for the diagnosis of bony Bankart (arrow) [Courtesy of prof. Carlo Faletti]

Ultrasonography

In clinical practice, the ultrasound examination is typically not used to assess shoulder instability [7]. Ultrasonography (US) is useful in the study of the rotator cuff pathology; the rotator

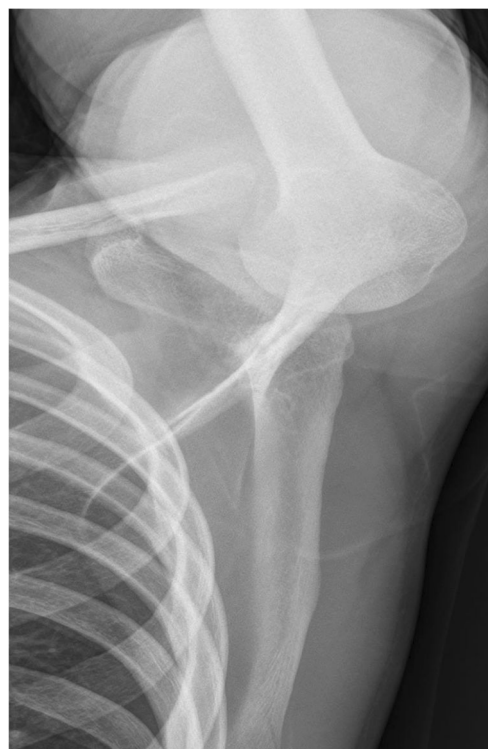


Fig. 13 CR, Stryker-Notch’s view image allows looking at the posterolateral aspect of the humeral head; in this case, the normal intersection of the profiles of the scapular glenoid and humeral head is shown

cuff is the main dynamic stabilizer of the shoulder. Acute cuff tears occur commonly in patients over 40 years with traumatic dislocation. However, ultrasound does not allow assessment of the static stabilizers, such as the glenoid labrum and glenohumeral ligaments [7].

Magnetic Resonance

Magnetic resonance examination in shoulder instability allows an accurate assessment of both static and dynamic stabilizers, in particular, of the capsular-labral complex and of the rotator cuff tendons [51, 52]. The image acquisition is obtained with high magnetic field devices (1–3 Tesla), equipped with dedicated surface coils, small field of view, and 2–4 mm thick slices. The field of view should include the acromion, entire humeral head, and scapula. The acquisitions are made in the three anatomical planes orthogonal to the longitudinal axis of the glenoid: axial, oblique coronal, and oblique sagittal [53].

The MRI examination in standard scans can be integrated with additional sequences that improve diagnostic accuracy for specific lesions based on clinical suspicion. In particular, the ABER position acquisitions (abduction extra-rotation of the arm) tenses the capsular-labral complex and allows a better evaluation for suspected Perthes lesion, longitudinal tears of the rotator cuff, and peel back lesions of the superoposterior labrum, whereas the ADIR position acquisitions (adduction internal rotation of the arm) can facilitate the identification of an ALPSA lesion [54–57].

Many MRI protocols for the evaluation of the unstable shoulder are available in the literature [52–54]; however, the fluid-sensitive sequences with fat suppression (TSE T2 fat-sat and PD fat-sat) are recognized as the best MRI protocol; the TSE T2 fat-sat and PD fat-sat allow accurate assessment of the capsular-labral complex and musculotendinous structures, and highlight bone edema, bursal distention, and paralabral cysts, if present [53, 58]. Concerning the labrum, it is usually triangular, meniscoid, or bumper with a low signal intensity attached to hyaline articular cartilage that usually presents an intermediate signal intensity on T1-weighted and T2-weighted MR images. Normal glenohumeral articular hyaline cartilage can simulate a superior or anterosuperior labral tear depicted as an area of linear high signal intensity placed between the labrum and glenoid fossa. Cartilage signal intensity is not usually as high as that of fluid or contrast medium within a tear. Moreover, it is important to evaluate if any anatomical variants such as Buford complex, sublaxal foramen, and sublaxal recess are present. Knowledge of normal chondral anatomy and signal characteristics is necessary to avoid overcalling a labral tear. Glenohumeral ligament (superior, middle, and inferior) tears can be seen as an increase in signal intensity on fluid-sensitive sequences with fat suppression

[59, 60]. The superior glenohumeral ligament is best investigated on axial images obtained exactly beneath or adjacent to the origin of the long head of the biceps tendon [9]. Superior glenohumeral ligament thickening may be seen along with absence or hypoplasia of the middle glenohumeral ligament and should not be mistaken for a remote injury. The middle glenohumeral ligament can be absent in up to 27% of individuals [61]. However, absence of this ligament is not associated with increased incidence of instability. On axial plane, it presents an oblique course whereas on oblique sagittal plane is in front of the glenoid. The inferior glenohumeral ligament consists of two bands: anterior and posterior. The anterior band is usually thicker than the posterior. In particular, the acquisition in oblique sagittal plane is useful for the evaluation of the inferior glenohumeral ligament and its attachments especially to avoid over diagnosing tear if the anterior band presents an anomalously high insertion from above 3-o'clock position of the anterosuperior labrum [62]. Labrum and glenohumeral ligaments are shown in Fig. 2.

Joint effusion, bursitis and paralabral cysts can be identified by these sequences demonstrating high signal intensity. The identification of paralabral cysts is important because they can compress the suprascapular nerve at the spino-glenoid notch with associated abnormal signal of the infraspinatus muscle. Failure to diagnose this condition can lead to delayed atrophy of the rotator cuff and periscapular muscles [58, 63, 64]. Ganglion cysts associated with anterior-inferior labral lesions may compress the axillary nerve at the level of the quadrilateral space and sometimes can extend to the bone, resulting in bone cysts [56, 57, 63].

The diagnostic accuracy of MRI in the assessment of shoulder instability can be increased by injecting contrast



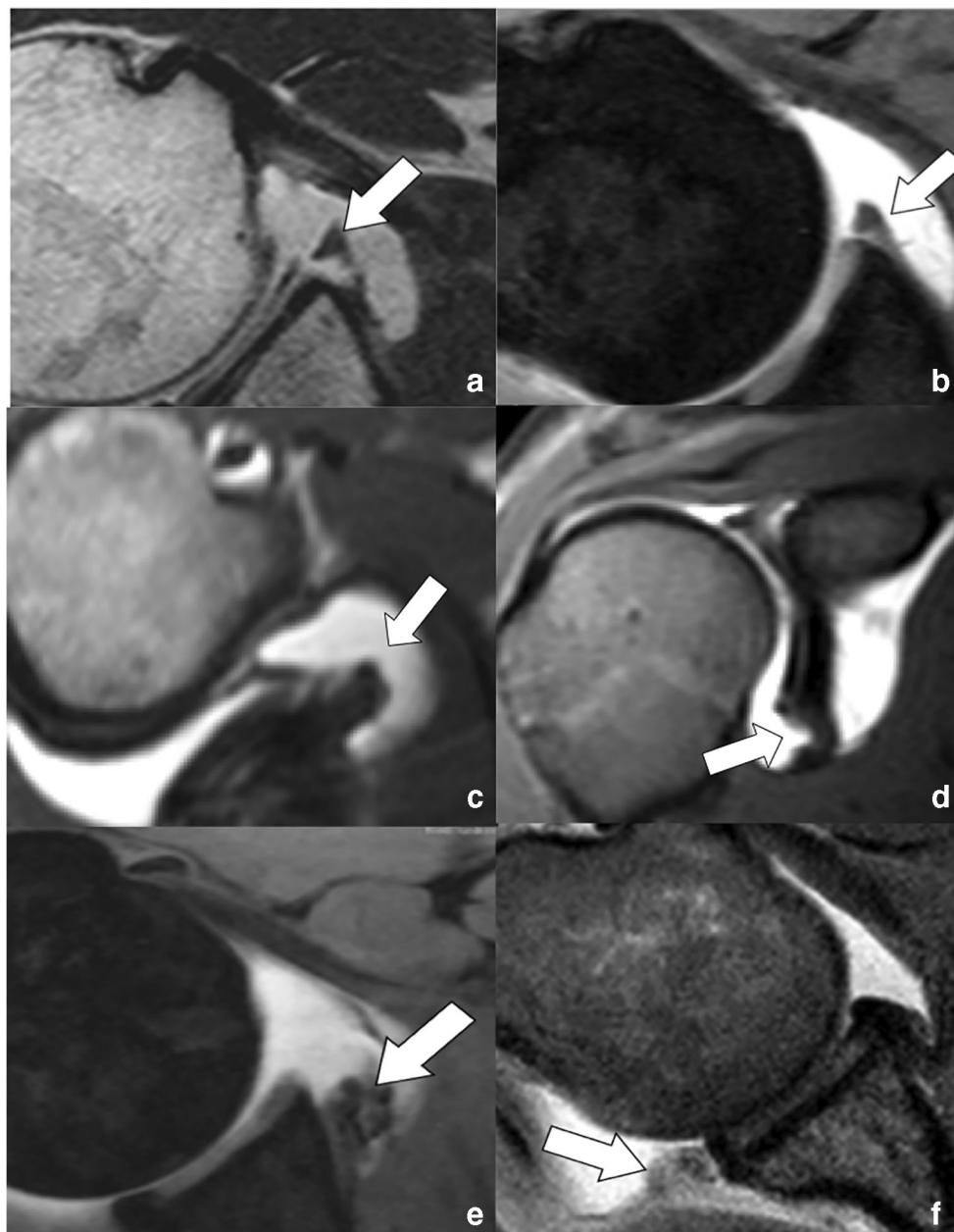
Fig. 14 Axial T1w Fat-saturated MR Arthrography image is the most suitable plan for the evaluation of the capsular type. In this image type III insertion that can lead to instability is shown (arrow). See Fig. 3 to get a schematic view of capsular insertion type

medium into the joint cavity (MR arthrography) [65]. The introduction of contrast medium into the glenohumeral joint, using the anterior or posterior approach, can be performed under fluoroscopic guidance, ultrasound or freehand, depending on experience and on the operator's preference [66, 67]. The injected material is a mixture of saline and Gadolinium; the latter reduces the T1 relaxation times and increase signal intensity on T1-weighted sequences. Injection of contrast medium is followed by the acquisition of T1-weighted sequences or T1 fat-sat. MR arthrography has many advantages over conventional MRI [2, 68, 69]. The most relevant are high spatial resolution, high signal to noise ratio; better definition of morphology, anatomical variants, and lesions of the glenoid

labrum and glenohumeral ligaments; evaluation of the capsular type, following distension of the joint cavity allows better visualization of loose bodies; better definition of possible partial tears of the rotator cuff tendons given by the spread of the contrast agent through the disrupted fibers (rotator cuff lesions more often originate from the articular side); reduced acquisition times compared with the use of T1-weighted sequences.

MR arthrography is indicated in patients with clinical manifestations of instability when the conventional MRI is not diagnostic; in these cases, MR arthrography allows an accurate tear identification and characterization of the capsular type (Fig. 14), glenoid labrum (Fig. 15) and glenohumeral ligament lesions (Figs. 16 and 17), consequently is the most

Fig. 15 a–f MR arthrography images showing different types of subequatorial fibrocartilaginous tears. **a** Axial T1 w image shows Bankart lesion (arrow); **b** axial T1 w SPIR image showing Perthes lesion (arrow); **c** axial T1w and **d** coronal T1w images showing ALPSA lesion (arrows); **e** axial T1 w SPIR image shows the glenoid labrum ovoid mass sign (GLOM) that indicates a torn anterior glenoid labrum that is retracted medially (arrow); **f** axial T1w SPIR image shows posterior labrum tear (arrow). See Fig. 4 for a schematic view of labral lesions



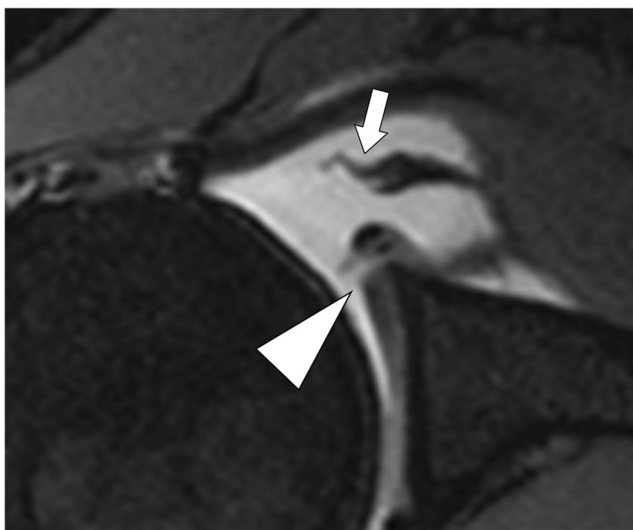


Fig. 16 Axial T1w Fat-suppressed MR arthrography image. This view is useful for the evaluation of inferior glenohumeral ligament rupture (arrow); note the presence of coexistent Perthes lesion (arrowhead)

accurate technique for the evaluation of the extent of damage [70–72].

In particular, the contrast agent distribution in labral lesions allows a better visualization and help in distinguishing them from the uncommon anatomical labral variants (Fig. 15) [40, 70, 71].

The subequatorial labral lesions should be evaluated in the axial slices, whereas SLAP lesions should be evaluated in the oblique coronal slices.

MR arthrography allows an accurate assessment of SLAP lesions and rotator interval (Fig. 18) [41]. The avulsion of the anterosuperior labrum is characterized by the presence of a high intensity signal line between fibrocartilaginous labrum and glenoid [29].

The abnormal hypersignal extends both anterior and posterior to the insertion of the biceps tendon on the labrum [9, 28, 29]. MR arthrography plays an important role in the

differentiation of the SLAP lesions from many anatomical variants that affect the anterosuperior labrum region (e.g., detachment of the superior labrum vs sublateral foramen; type II SLAP lesion vs sublateral recess) [10, 13, 40]. The distinction between labral lesions and sublateral recess anatomy is based on the orientation of the high signal intensity line in coronal sections; in the labral lesions (i.e., type II SLAP), the hyperintensity orientation is directed laterally, whereas in sublateral recess the orientation is medial (Fig. 15b) [10, 40, 41]. Waldt's study reports an accuracy of MR arthrography evaluation of Perthes lesion of 50%, especially in the presence of fibrotic phenomena that prevent the distribution of the contrast medium in the joint cavity [51]. In this case, the diagnostic accuracy of MR arthrography could be improved with the arm in ABER position [54].

The isolated humeral avulsion of the inferior glenohumeral ligament can be evaluated in oblique coronal MR arthrography images; the ligamentous disconnection is usually on the humeral side (poorly detectable in arthroscopy) configuring the arthro-MRI “J sign” in contrast to the normal U-shaped inferior glenohumeral recess (Fig. 17).

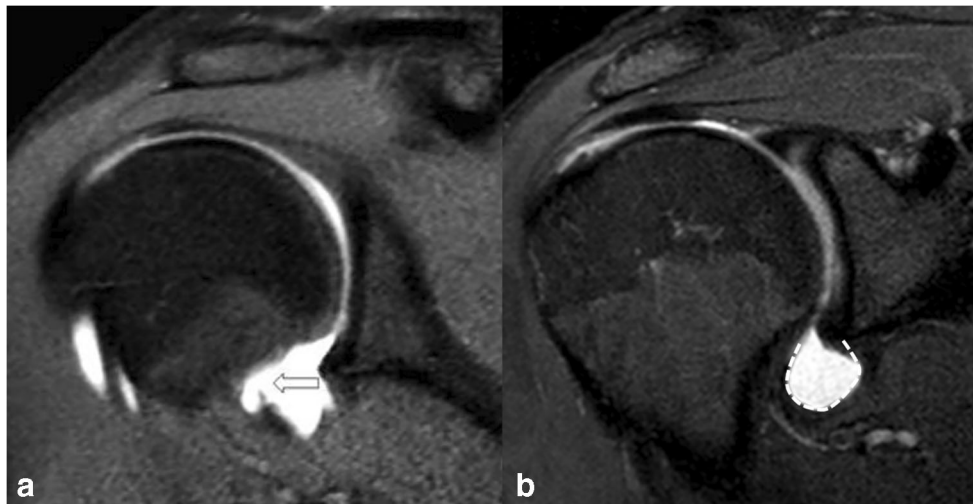
In addition to the study of shoulder instability, MR arthrography is also indicated in the evaluation of operated shoulders, in adhesive capsulitis, and in the demonstration of small and dubious partial tears of the rotator cuff [5, 52, 68, 69].

Computed Tomography

Computed tomography is indicated in patients with shoulder instability for the assessment of bone lesions, above all to quantify the deficit of the glenoid bone surface (bone loss) [65, 73].

CT arthrography is indicated for patients with absolute or relative contraindications (electrical subcutaneous implants

Fig. 17 a, b Oblique coronal SE T1w SPIR MR Arthrography images in two different shoulders. In **a**, outcome of humeral avulsion of the glenohumeral ligament is shown, poorly detectable in arthroscopy, is seen as the arthro-MRI “J sign” (arrow) unlike the normal U-shaped inferior glenohumeral recess (**b**, dashed line)



such pacemakers, permanent defibrillators, etc.) to the MRI study or with surgical articular artifacts (due to metal implants) even if it not very frequent nowadays; however, in these patients, CT arthrography evaluation represents an effective diagnostic alternative to MRI, for example, in the assessment of SLAP lesion with an accuracy comparable to that of MR arthrography (Fig. 19) [46, 53, 73]. Moreover, the presence of ferromagnetic dust released during joint surgeries can significantly reduce the quality of MRI images and justify a CT arthrography study [46, 53, 67].

The MDCT technology (multidetector spiral CT) has the advantage of high spatial resolution and isotropic volumes. This allows high-quality retrospective image reconstruction on each plane. Moreover, the injection of contrast medium in the joint enhances the contrast resolution, therefore some authors prefer CT arthrography for the study of micro and macro shoulder instability [46, 74].

CT is essential in the evaluation of shoulder macroinstability in order to quantify glenoid bone loss [65]. The glenoid deficit (“bone loss”) is defined as the reduction of the glenoid surface, which may be a consequence of bone fractures (bony Bankart

or glenoid erosions in turn determined by the friction between the humeral head and glenoid margin in patients with recurrent dislocations [22, 65, 74, 75].

According to Burkhart et al., a bone deficit greater than 25% correlates with a high rate (67%) of recurrent dislocation, while for minor defects, the percentage decreases to 4% [76, 77]. This is based on the inverted pear shape of the glenoid fossa on CT and MR. This appearance of the glenoid requires a defect of a minimum of 25% of the bone width of the inferior glenoid. There are multiple additional techniques of measuring glenoid bone loss. For example, a technique proposed by Griffith et al. measures the difference between the maximum width of the glenoid fossa in the injured and the contralateral shoulder. Another technique proposed by the same authors measures a maximum glenoid width to length ratio. The flattened anterior glenoid results in a decreased ratio. The best-fit circle method is another technique used, based on measuring glenoid bone defects on sagittal views. The Pico method was described by Baudi et al. and is performed by measuring two circles on the injured and contralateral healthy glenoid, the missing segment of the circle on the injured glenoid is measured. This is calculated as

Fig. 18 a–d Coronal MR arthrography SE T1w SPIR images showing SLAP lesions. In **a** type I, fraying of superior labrum without contrast medium infiltration; in **b** type II, showing a globular area of contrast medium penetration in the superior labrum; in **c** type III, presenting with “bucket handle” lesion of the upper portion of the labrum without extension into biceps tendon; in **d** type IV, type III with involvement of biceps tendons. See Fig. 7 to get a schematic view of SLAP lesions

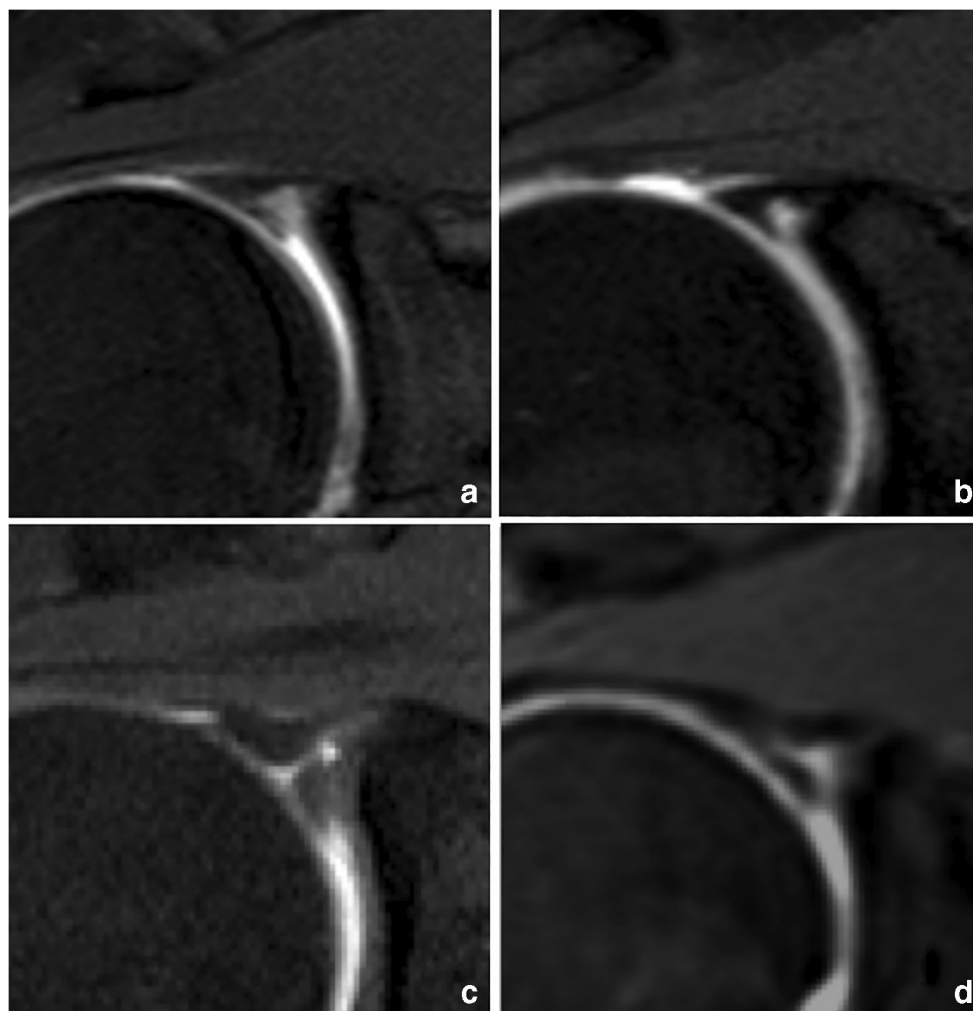


Fig. 19 CT arthrography is indicated for patients with surgical outcome with ferromagnetic devices or with absolute contraindication to MRI examination as an effective alternative imaging technique for shoulder instability. (a, b) Oblique multiplanar reconstruction (MPR) CT arthrography images showing **a** type II SLAP lesion before surgery; **b** recurrence of type IV SLAP lesion after surgery (note the two metallic anchors in the scapular Glena)



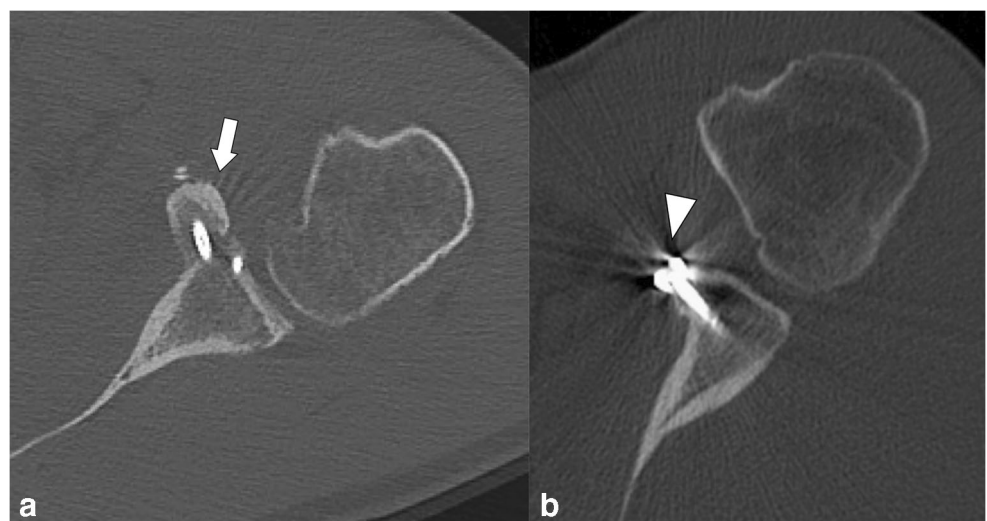
the surface $D/\text{surface } A \times 100$ where surface D is the size of the defect and surface A is the size of the contralateral healthy glenoid [78]. In a previous study, the inter-observer variability for CT measurement of the glenoid surface using the CT Pico method was high when compared with the reference standard (laser), in the assessment of glenoid surface in cadaveric specimens, thus the CT Pico method is not reliable and could cause errors in the clinical management of the patient [78, 79].

The presence of glenoid bone deficit of at least 25% excludes the possibility of recovering the stability by arthroscopy and indicates that a more invasive arthrotomic treatment is required, according to the Latarjet-Putti procedure (Fig. 20) [80]. The procedure consists of the removal and transfer of a section of the coracoid process and its attached muscles (short head of biceps, coracobrachial ligament) to the anteroinferior glenoid. This placement of the coracoid acts as a bone block which together with the transferred muscles prevent further dislocation of the joint. The attached tendons provide additional support reducing the propensity for damage to the anterior-inferior joint capsule and recurrent shoulder dislocation.

Therefore, the accurate quantification of the bone loss by CT is crucial for a correct pre-operative planning and for the assessment of recurrent shoulder dislocation after surgery [46, 75].

The best CT method to calculate the glenoid bone loss is the multiplanar curve reconstructions (cMPR); this method guarantees higher accuracy and minimizes inter-observer variability compared with other methods [76, 81]. A flat oblique sagittal reconstruction is used to obtain a measurement of the articular glenoid surface. A flat oblique sagittal reconstruction oriented on the articular glenoid surface is obtained according to the best-fitting plane showing the whole glenoid surface (including external borders). The reconstructions obtained allow measuring the total glenoid surface area using a hand-drawn perimeter (region of interest [ROI]) along the external borders of the articular glenoid surface. The curved multiplanar reconstruction (cMPR) is used to obtain a plane overlapping the glenoid surface. The cMPR is traced on an oblique coronal plane to seek the glenoid articular surface concavity. Finally, the reconstructions obtained enable to measure the total glenoid surface area using a hand-drawn

Fig. 20 **a, b** Axial CT images shows Latarjet-Putti procedure. In **a**, note the bone block system made by the coracoid process (arrow) positioned in the anteroinferior glenoid process providing a barrier to the anterior translation of the humeral head. In **b**, failure of the bone block system given by the bone resorption (arrowhead).



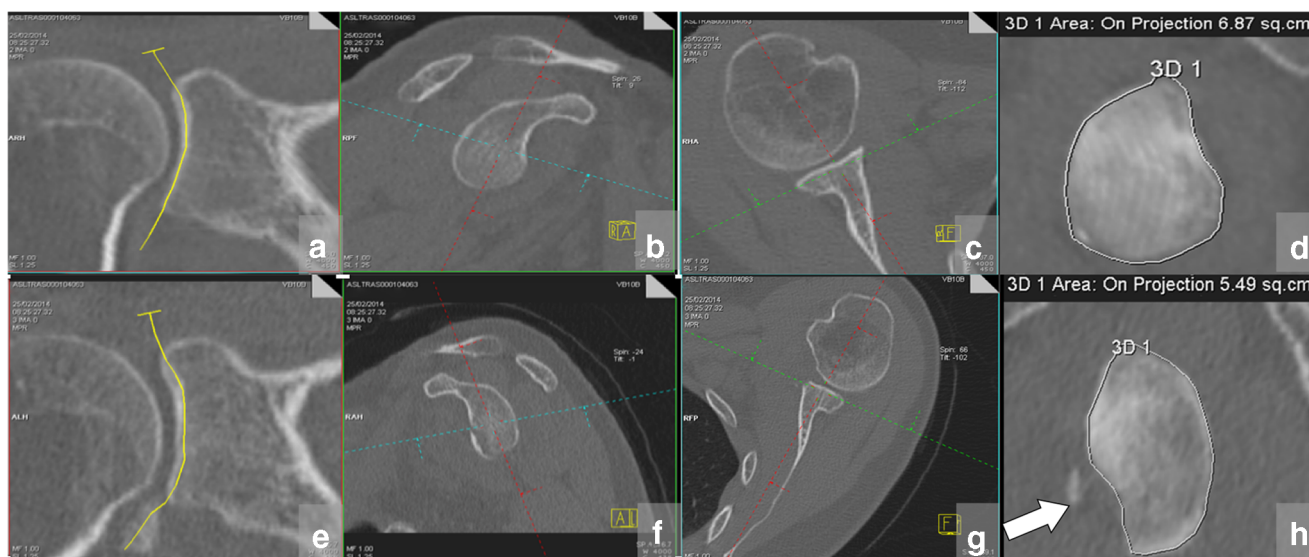


Fig. 21 a–h Curved MPR CT images is an accurate and reproducible method of assessing bone loss in order to determine the glenoid surface. Note the glenoid surface calculation by curved MPR in the healthy shoulder (a–d) and in the unstable shoulder (e–h). Comparison between

the healthy scapular Glena with a surface of 6.87 cm² (d) and the contralateral unstable shoulder Glena with a surface of 5.49 cm² (h), with bone loss and bony Bankart lesion (arrow)

ROI along the external borders of the articular glenoid surface (Fig. 21).

CT evaluation allows an accurate assessment of Hill-Sachs and Hill-Sachs reverse lesions. The selection of the surgical treatment for restoring glenohumeral joint stability depends on the presence or absence of the glenoid bone loss, as well as the position of Hill-Sachs lesions. As previously mentioned, the Hill-Sachs lesions, when affecting the apex of the humeral head and fitting in the “glenoid track” (Fig. 5), are responsible for the high rate of recurrent dislocation after arthroscopic treatment of capsuloplasty, and typically require other surgical techniques such as the arthroscopic remplissage or Latarjet [31].

Volume rendering reconstructions are particularly useful in the evaluation of the course of Hill-Sachs lesions, as these reconstructions provide panoramic views (Fig. 22).

Some recent studies have investigated the possibility of evaluating bone lesions using MRI [82].

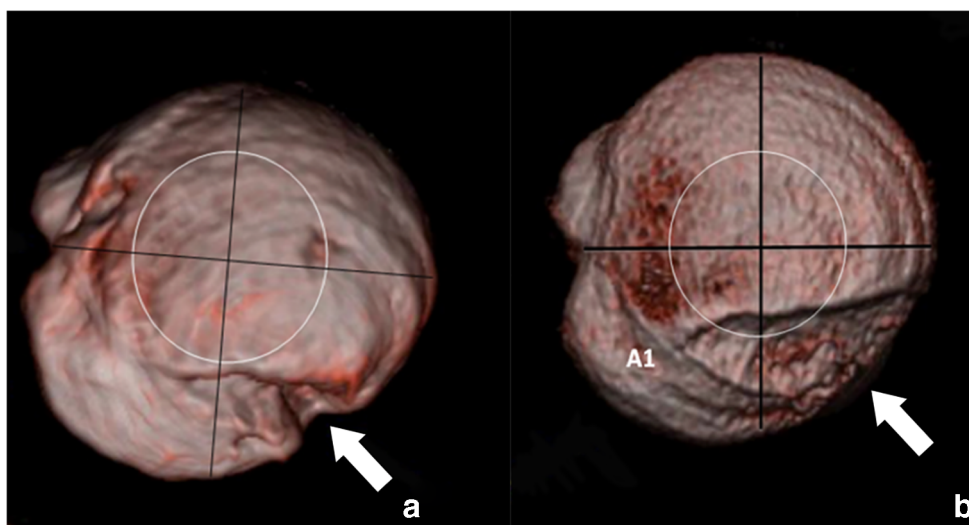
All of the previous imaging techniques are also useful in evaluation and management of postoperative shoulder instability [83, 84].

Conclusions

The diagnosis of shoulder instability is clinical; however, the radiological imaging contributes significantly to the therapeutic planning by identifying the anatomical conditions predisposing to shoulder instability and extent of associated injuries [6–8].

Conventional radiology is a first level exam in the evaluation of shoulder instability; certain radiographic projections

Fig. 22 a–b Volume Rendering reconstructions CT images showing the orientation of Hill-Sachs lesions: a vertical lesion (arrow); b horizontal lesion (arrow). Hill-Sachs lesions, when fitting in the “glenoid track” or affecting the area next to the apex of the humeral head, are responsible for the high rate of recurrent dislocation after arthroscopic treatment of capsuloplasty and typically require other surgical techniques such as the arthroscopic remplissage or Latarjet technique



allow accurate assessment of the glenohumeral joint, specifically its articular and osseous components. Ultrasonography plays a minor role in the diagnostic evaluation of shoulder instability, useful mainly in the evaluation of potential associated rotator cuff injuries.

Magnetic resonance allows an evaluation of the rotator cuff tendons, the glenohumeral and AC joints, and surrounding bursae. Edema and possible glenohumeral fractures associated may be evaluated. The diagnostic accuracy of MRI can be enhanced with the arthrography technique.

Specifically, many authors have agreed that MR arthrography investigation is more accurate in the identification and quantification of the damage of the capsuloligamentous complex than MRI on its own. Moreover, it plays an important role in postoperative evaluation of patients with a clinical diagnosis of instability. Computed tomography is indicated for the assessment of bone lesions, and in particular for the quantification of glenoid bone loss in patients with shoulder instability.

CT arthrography is indicated for patients with absolute or relative contraindications to the MRI study (pacemakers, subcutaneous defibrillators, etc.). It may also serve as an effective diagnostic alternative in cases where ferromagnetic surgical materials would limit effective MR evaluation. However, some authors prefer CT arthrography for the study of micro and macro shoulder instability due to high spatial and contrast resolution.

Compliance with ethical standards

Conflict of interest The authors declare that they have no conflict of interest.

References

- Jaggi A, Noorani A, Malone A, Cowan J, Lambert S, Bayley I. Muscle activation patterns in patients with recurrent shoulder instability. *Int J Shoulder Surg.* 2012;6(4):101–7.
- Pastor MF, Smith T, Struck M, Wellmann M. Stability versus mobility of the shoulder. *Biomechanical aspects in athletes.* *Orthopade.* 2014;43(3):209–14.
- Gerber C, Nyffeler RW. Classification of glenohumeral joint instability. *Clin Orthop Relat Res.* 2002;400:65–76.
- Myers JB, Oyama S. Sensorimotor factors affecting outcome following shoulder injury. *Clin Sports Med.* 2008;27(3):481–90 x.
- Matsen FA 3rd, Harryman DT 2nd, Sidles JA. Mechanics of glenohumeral instability. *Clin Sports Med.* 1991;10(4):783–8.
- Seeger LL, Gold RH, Bassett LW. Shoulder instability: evaluation with MR imaging. *Radiology.* 1988;168(3):695–7.
- Jacobson JA. Shoulder US: anatomy, technique, and scanning pitfalls. *Radiology.* 2011;260(1):6–16.
- Flannigan B, Kursunoglu-Brahme S, Snyder S, Karzel R, Del Pizzo W, Resnick D. MR arthrography of the shoulder: comparison with conventional MR imaging. *AJR Am J Roentgenol.* 1990;155(4):829–32.
- Steinbach LS. MRI of shoulder instability. *Eur J Radiol.* 2008;68(1):57–71.
- Tirman PF, Smith ED, Stoller DW, Fritz RC. Shoulder imaging in athletes. *Semin Musculoskelet Radiol.* 2004;8(1):29–40.
- Kadi R, Milants A, Shahabpour M. Shoulder anatomy and normal variants. *J Belg Soc Radiol.* 2017;101(Suppl 2):3.
- Williams MM, Snyder SJ. A sublateral foramen must not be confused with a Bankart lesion. *Arthroscopy.* 1994;10(5):586.
- Mohana-Borges AV, Chung CB, Resnick D. Superior labral anteroposterior tear: classification and diagnosis on MRI and MR arthrography. *AJR Am J Roentgenol.* 2003;181(6):1449–62.
- Reinold MM, Curtis AS. Microinstability of the shoulder in the overhead athlete. *Int J Sports Phys Ther.* 2013;8(5):601–16.
- Chan KK, Muldoon KA, Yeh L, Boutin R, Pedowitz R, Skaf A, et al. Superior labral anteroposterior lesions: MR arthrography with arm traction. *AJR Am J Roentgenol.* 1999;173(4):1117–22.
- Thomas SC, Matsen FA 3rd. An approach to the repair of avulsion of the glenohumeral ligaments in the management of traumatic anterior glenohumeral instability. *J Bone Joint Surg Am.* 1989;71(4):506–13.
- Schneeberger AG, Hersche O, Gerber C. The unstable shoulder. Classification and therapy. *Unfallchirurg.* 1998;101(3):226–31.
- Farrar NG, Malal JJ, Fischer J, Waseem M. An overview of shoulder instability and its management. *Open Orthop J.* 2013;7:338–46.
- Winge S, Thomsen NO, Jensen CH, Klareskov B. Shoulder instability. *Ugeskr Laeger.* 1998;160(25):3707–13.
- Sudkamp NP, Granrath M, Hoffmann R, Haas NP. Instability of the shoulder joint in the athlete. *Chirurg.* 1994;65(11):901–9.
- Ly JQ, Beall DP, Sanders TG. MR imaging of glenohumeral instability. *AJR Am J Roentgenol.* 2003;181(1):203–13.
- Wischer TK, Bredella MA, Genant HK, Stoller DW, Bost FW, Tirman PF. Perthes lesion (a variant of the Bankart lesion): MR imaging and MR arthrographic findings with surgical correlation. *AJR Am J Roentgenol.* 2002;178(1):233–7.
- Bernhardson AS, Bailey JR, Solomon DJ, Stanley M, Provencher MT. Glenoid bone loss in the setting of an anterior labroligamentous periosteal sleeve avulsion tear. *Am J Sports Med.* 2014;42(9):2136–40.
- Amrami KK, Sperling JW, Bartholmai BJ, Sundaram M. Radiologic case study. Glenolabral articular disruption (GLAD) lesion. *Orthopedics.* 2002;25(1):29 95–6.
- Bozzo A, Oitment C, Thomley P, Yan J, Habib A, Hoppe DJ, et al. Humeral avulsion of the glenohumeral ligament: indications for surgical treatment and outcomes—a systematic review. *Orthop J Sports Med.* 2017;5(8):2325967117723329.
- Kwak SM, Brown RR, Trudell D, Resnick D. Glenohumeral joint: comparison of shoulder positions at MR arthrography. *Radiology.* 1998;208(2):375–80.
- Wolf EM, Arianjan A. Hill-Sachs remplissage, an arthroscopic solution for the engaging Hill-Sachs lesion: 2-10-year follow-up and incidence of recurrence. *J shoulder Elb Surg.* 2014;23 (6):814–20
- Horst K, Von Harten R, Weber C, Andruszkow H, Pfeifer R, Dienstknecht T, et al. Assessment of coincidence and defect sizes in Bankart and Hill-Sachs lesions after anterior shoulder dislocation: a radiological study. *Br J Radiol.* 2014;87(1034):20130673.
- Rashid MS, Crichton J, Butt U, Akimau PI, Charalambous CP. Arthroscopic “Remplissage” for shoulder instability: a systematic review. *Knee Surg Sports Traumatol Arthrosc.* 2016;24(2):578–84.
- Maio M, Sarmiento M, Moura N, Cartucho A. How to measure a Hill-Sachs lesion: a systematic review. *EFORT Open Rev.* 2019;4(4):151–7.
- Yamamoto N, Itoi E, Abe H, Minagawa H, Seki N, Shimada Y, et al. Contact between the glenoid and the humeral head in abduction, external rotation, and horizontal extension: a new concept of glenoid track. *J Shoulder Elb Surg.* 2007;16(5):649–56.

32. Di Giacomo G, Itoi E, Burkhart SS. Evolving concept of bipolar bone loss and the Hill-Sachs lesion: from “engaging/non-engaging” lesion to “on-track/off-track” lesion. *Arthroscopy*. 2014;30(1):90–8.
33. Itoi E. ‘On-track’ and ‘off-track’ shoulder lesions. *EFORT Open Rev*. 2017;2(8):343–51.
34. Morsy MG. Arthroscopic remplissage: is it still an option? *EFORT Open Rev*. 2017;2(12):478–83.
35. Moussa ME, Boykin RE, Earp BE. Missed locked posterior shoulder dislocation with a reverse Hill-Sachs lesion and subscapularis rupture. *Am J Orthop (Belle Mead NJ)*. 2013;42(12):E121–4.
36. Park KJ, Jeong HS, Park JK, Cha JK, Kang SW. Evaluation of inferior capsular laxity in patients with atraumatic multidirectional shoulder instability with magnetic resonance arthrography. *Korean J Radiol*. 2019;20(6):931–8.
37. Castagna A, Nordenson U, Garofalo R, Karlsson J. Minor shoulder instability. *Arthroscopy*. 2007;23(2):211–5.
38. Garofalo R, Pouliart N, Vinci E, Franceschi G, Aldegheri R, Castagna A. Anterosuperior labral tear without biceps anchor involvement: a subtle isolated cause of a painful shoulder. *Arthroscopy*. 2011;27(1):17–23.
39. Castagna A, Delle Rose G, Borroni M, Markopoulos N, Conti M, Maradei L, et al. Modified MacLaughlin procedure in the treatment of neglected posterior dislocation of the shoulder. *Chir Organi Mov*. 2009;93(Suppl 1):S1–5.
40. Arai R, Kobayashi M, Harada H, Tsukiyama H, Saji T, Toda Y, et al. Anatomical study for SLAP lesion repair. *Knee Surg Sports Traumatol Arthrosc*. 2014;22(2):435–41.
41. Li HF, Liu YJ, Cheng LQ, Li ZL, Wang JL, Qi W, et al. Diagnostic value of MRI and MR arthrography in the detection of injuries of anterior labrum in shoulder. *Zhongguo Gu Shang*. 2012;25(5):413–7.
42. Vogel LA, Moen TC, Macaulay AA, Arons RR, Cadet ER, Ahmad CS, et al. Superior labrum anterior-to-posterior repair incidence: a longitudinal investigation of community and academic databases. *J Shoulder Elb Surg*. 2014;23(6):e119–26.
43. Snyder SJ, Karzel RP, Del Pizzo W, Ferkel RD, Friedman MJ. SLAP lesions of the shoulder. *Arthroscopy*. 1990;6(4):274–9.
44. Barile A, Lanni G, Conti L, Mariani S, Calvisi V, Castagna A, et al. Lesions of the biceps pulley as cause of anterosuperior impingement of the shoulder in the athlete: potentials and limits of MR arthrography compared with arthroscopy. *Radiol Med*. 2013;118(1):112–22.
45. Genovese E, Spano E, Castagna A, Leonardi A, Angeretti MG, Callegari L, et al. MR-arthrography in superior instability of the shoulder: correlation with arthroscopy. *Radiol Med*. 2013;118(6):1022–33.
46. De Filippo M, Araoz PA, Pogliacomini F, Castagna A, Petriccioli D, Sverzellati N, et al. Recurrent superior labral anterior-to-posterior tears after surgery: detection and grading with CT arthrography. *Radiology*. 2009;252(3):781–8.
47. Ek ET, Shi LL, Tompson JD, Freehill MT, Warner JJ. Surgical treatment of isolated type II superior labrum anterior-posterior (SLAP) lesions: repair versus biceps tenodesis. *J Shoulder Elb Surg*. 2014;23(7):1059–65.
48. Wijdicks CA, Anavian J, Hill BW, Armitage BM, Vang S, Cole PA. The assessment of scapular radiographs: analysis of anteroposterior radiographs of the shoulder and the effect of rotational offset on the glenopolar angle. *Bone Joint J*. 2013;95-B(8):1114–20.
49. Wagner E, Arditi D, Guerne PA, Lanier C. Diagnostic imaging for atraumatic shoulder pain. *Rev Med Suisse*. 2013;9(399):1726–31.
50. Murachovsky J, Bueno RS, Nascimento LG, Almeida LH, Strose E, Castiglia MT, et al. Calculating anterior glenoid bone loss using the Bernageau profile view. *Skelet Radiol*. 2012;41(10):1231–7.
51. Woertler K, Waldt S. MR imaging in sports-related glenohumeral instability. *Eur Radiol*. 2006;16(12):2622–36.
52. Steinbach LS. Magnetic resonance imaging of glenohumeral joint instability. *Semin Musculoskelet Radiol*. 2005;9(1):44–55.
53. Hodler J, Kursunoglu-Brahme S, Snyder SJ, Cervilla V, Karzel RP, Schweitzer ME, et al. Rotator cuff disease: assessment with MR arthrography versus standard MR imaging in 36 patients with arthroscopic confirmation. *Radiology*. 1992;182(2):431–6.
54. Tian CY, Cui GQ, Zheng ZZ, Ren AH. The added value of ABER position for the detection and classification of anteroinferior labroligamentous lesions in MR arthrography of the shoulder. *Eur J Radiol*. 2013;82(4):651–7.
55. Song HT, Huh YM, Kim S, Lee SA, Kim SJ, Shin KH, et al. Anterior-inferior labral lesions of recurrent shoulder dislocation evaluated by MR arthrography in an adduction internal rotation (ADIR) position. *J Magn Reson Imaging*. 2006;23(1):29–35.
56. Kreitner KF, Botchen K, Rude J, Bittinger F, Krummenauer F, Thelen M. Superior labrum and labral-bicipital complex: MR imaging with pathologic-anatomic and histologic correlation. *AJR Am J Roentgenol*. 1998;170(3):599–605.
57. Bowen MK, Warren RF. Ligamentous control of shoulder stability based on selective cutting and static translation experiments. *Clin Sports Med*. 1991;10(4):757–82.
58. Zlatkin MB, Sanders TG. Magnetic resonance imaging of the glenoid labrum. *Radiol Clin N Am*. 2013;51(2):279–97.
59. Chandnani VP, Yeager TD, DeBerardino T, Christensen K, Gagliardi JA, Heitz DR, et al. Glenoid labral tears: prospective evaluation with MRI imaging, MR arthrography, and CT arthrography. *AJR Am J Roentgenol*. 1993;161(6):1229–35.
60. Palmer WE, Brown JH, Rosenthal DI. Labral-ligamentous complex of the shoulder: evaluation with MR arthrography. *Radiology*. 1994;190(3):645–51.
61. Beltran J, Bencardino J, Mellado J, Rosenberg ZS, Irish RD. MR arthrography of the shoulder: variants and pitfalls. *Radiographics*. 1997;17(6):1403–12 discussion 12–5.
62. Motamedi D, Everist BM, Mahanty SR, Steinbach LS. Pitfalls in shoulder MRI: part 1—normal anatomy and anatomic variants. *AJR Am J Roentgenol*. 2014;203(3):501–7.
63. Westrick RB, Fogarty BT, Johnson MP. Posterior labral tear with a paralabral cyst causing suprascapular nerve compression. *J Orthop Sports Phys Ther*. 2013;43(7):511.
64. Limbucci N, Rossi F, Salvati F, Pistoia LM, Barile A, Masciocchi C. Bilateral suprascapular nerve entrapment by glenoid labral cysts associated with rotator cuff damage and posterior instability in an amateur weightlifter. *J Sports Med Phys Fitness*. 2010;50(1):64–7.
65. Rhee RB, Chan KK, Lieu JG, Kim BS, Steinbach LS. MR and CT arthrography of the shoulder. *Semin Musculoskelet Radiol*. 2012;16(1):3–14.
66. O’Connell PW, Nuber GW, Mileski RA, Lautenschlager E. The contribution of the glenohumeral ligaments to anterior stability of the shoulder joint. *Am J Sports Med*. 1990;18(6):579–84.
67. Faletti C, De Filippo M, Giudice G, Larciprete M, Seccia A, Regis G. Fibro-cartilaginous lesions of the glenoid labrum in shoulder instability: a proposed classification using sagittal-oblique arthro-MRI. *Radiol Med*. 2002;104(1–2):68–74.
68. Chandnani VP, Gagliardi JA, Murnane TG, Bradley YC, DeBerardino TA, Spaeth J, et al. Glenohumeral ligaments and shoulder capsular mechanism: evaluation with MR arthrography. *Radiology*. 1995;196(1):27–32.
69. Palmer WE, Caslowitz PL. Anterior shoulder instability: diagnostic criteria determined from prospective analysis of 121 MR arthrograms. *Radiology*. 1995;197(3):819–25.
70. Willemssen UF, Wiedemann E, Brunner U, Scheck R, Pfluger T, Kueffer G, et al. Prospective evaluation of MR arthrography performed with high-volume intraarticular saline enhancement in

- patients with recurrent anterior dislocations of the shoulder. *AJR Am J Roentgenol.* 1998;170(1):79–84.
71. Hajek PC, Sartoris DJ, Neumann CH, Resnick D. Potential contrast agents for MR arthrography: in vitro evaluation and practical observations. *AJR Am J Roentgenol.* 1987;149(1):97–104.
 72. Radwan A, Francis J, Green A, Kahl E, Maciurzynski D, Quartulli A, et al. Is there a relation between shoulder dysfunction and core instability? *Int J Sports Phys Ther.* 2014;9(1):8–13.
 73. Noonan B, Hollister SJ, Sekiya JK, Bedi A. Comparison of reconstructive procedures for glenoid bone loss associated with recurrent anterior shoulder instability. *J Shoulder Elb Surg.* 2014;23(8):1113–9.
 74. De Filippo M, Bertellini A, Sverzellati N, Pogliacomini F, Costantino C, Vitale M, Zappia M, Corradi D, Garlaschi G, Zompatori. Multidetector computed tomography arthrography of the shoulder: diagnostic accuracy and indications. *Acta Radiol.* 2008 Jun;49(5):540–9. <https://doi.org/10.1080/02841850801935559>.
 75. De Filippo M, Castagna A, Steinbach LS, Silva M, Concaro G, Pedrazzi G, et al. Reproducible noninvasive method for evaluation of glenoid bone loss by multiplanar reconstruction curved computed tomographic imaging using a cadaveric model. *Arthroscopy.* 2013;29(3):471–7.
 76. Provencher MT, Bhatia S, Ghodadra NS, Grumet RC, Bach BR Jr, Dewing CB, et al. Recurrent shoulder instability: current concepts for evaluation and management of glenoid bone loss. *J Bone Joint Surg Am.* 2010;92(Suppl 2):133–51.
 77. Waldt S, Burkart A, Imhoff AB, Bruegel M, Rummeny EJ, Woertler K. Anterior shoulder instability: accuracy of MR arthrography in the classification of antero-inferior labroligamentous injuries. *Radiology.* 2005;237(2):578–83.
 78. Skupinski J, Piechota MZ, Wawrzynek W, Maczuch J, Babinska A. The bony Bankart lesion: how to measure the glenoid bone loss. *Pol J Radiol.* 2017;82:58–63.
 79. De Filippo M, Saba L, Negrini G, Silva M, Pedrazzi G, Pogliacomini F, et al. Inter-observer agreement of CT measurement of the glenoid bone surface by the CT Pico method: comparison with laser in a cadaveric model. *Skelet Radiol.* 2015;44(10):1491–7.
 80. Ahmad CS, Freehill MQ, Blaine TA, Levine WN, Bigliani LU. Anteromedial capsular redundancy and labral deficiency in shoulder instability. *Am J Sports Med.* 2003;31(2):247–52.
 81. Huijsmans PE, Haen PS, Kidd M, Dhert WJ, van der Hulst VP, Willems WJ. Quantification of a glenoid defect with three-dimensional computed tomography and magnetic resonance imaging: a cadaveric study. *J Shoulder Elb Surg.* 2007;16(6):803–9.
 82. Gyftopoulos S, Beltran LS, Yemin A, Strauss E, Meislin R, Jazrawi L, et al. Use of 3D MR reconstructions in the evaluation of glenoid bone loss: a clinical study. *Skelet Radiol.* 2014;43(2):213–8.
 83. Barile A, Bruno F, Mariani S, Arrigoni F, Reginelli A, De Filippo M, et al. What can be seen after rotator cuff repair: a brief review of diagnostic imaging findings. *Musculoskelet Surg.* 2017;101(Suppl 1):3–14.
 84. De Filippo M, Pesce A, Barile A, Borgia D, Zappia M, Romano A, et al. Imaging of postoperative shoulder instability. *Musculoskelet Surg.* 2017;101(Suppl 1):15–22.

Publisher's note Springer Nature remains neutral with regard to jurisdictional claims in published maps and institutional affiliations.